Specific binding of endocrine transforming growth factor-beta 1 to vascular endothelium.

K Dickson, … , M O'Connor-McCourt, J J Bergeron

J Clin Invest. 1995;95(6):2539-2554. https://doi.org/10.1172/JCI117955.

Research Article

The presentation of recombinant biologically active 125I-TGF-beta 1 via the bloodstream to potential target cells in mice and rats was evaluated by quantitative light and electron microscope radioautography. Specificity was evaluated by in vivo competition with excess unlabeled TGF-beta 1, and integrity of the ligand at the binding site was demonstrated by trichloroacetic acid precipitation after extraction from tissues. The distribution of radiolabel at 2.5, 15, 30, 45, and 60 min after 125I-TGF-beta 1 injection revealed radiolabel principally over microvasculature endothelium but at times > 2.5 min over endothelial endocytic components indicative of internalization. Nonspecific binding of 125I-TGF-beta 1 to the apex of the proximal convoluted tubule of the kidney indicated it as the likely site of rapid clearance of TGF-beta 1 from the circulation, while a comparison of the binding of 125I-TGF-beta 1 (endothelial) to that of 125I-TGF-beta 1 complexed with alpha 2-macroglobulin-methylamine (liver parenchyma) indicated that clearance of TGF-beta 1 complexed alpha 2-macroglobulin was likely via the hepatic alpha 2-macroglobulin receptor. The endothelial TGF-beta receptors uncovered here are likely involved in the local regulatory mechanism of leukocyte and monocyte adhesion and tissue infiltration regulated by endocrine TGF-beta 1.

Specific Binding of Endocrine Transforming Growth Factor-β1 to Vascular Endothelium

K. Dickson,* A. Philip,‡ H. Warshawsky,* M. O'Connor-McCourt,‡ and J. J. M. Bergeron*
**Department of Anatomy and Cell Biology, McGill University, Montreal, Quebec H3A 2B2, and ‡Biotechnology Research Institute, Montreal, Quebec H4P 2R2, Canada*

Abstract

The presentation of recombinant biologically active ^{125}I-TGF-β1 via the bloodstream to potential target cells in mice and rats was evaluated by quantitative light and electron microscope radioautography. Specificity was evaluated by in vivo competition with excess unlabeled TGF-β1, and integrity of the ligand at the binding site was demonstrated by trichloroacetic acid precipitation after extraction from tissues. The distribution of radiolabel at 2.5, 15, 30, 45, and 60 min after ^{125}I-TGF-β1 injection revealed radiolabel principally over microvasculature endothelium but at times > 2.5 min over endothelial endocytic components indicative of internalization. Nonspecific binding of ^{125}I-TGF-β1 to the apex of the proximal convoluted tubule of the kidney indicated it as the likely site of rapid clearance of TGF-β1 from the circulation, while a comparison of the binding of ^{125}I-TGF-β1 (endothelial) to that of ^{125}I-TGF-β1 complexed with α_2-macroglobulin–methylamine (liver parenchyma) indicated that clearance of TGF-β1 complexed α2-macroglobulin was likely via the hepatic α2-macroglobulin receptor. The endothelial TGF-β receptors uncovered here are likely involved in the local regulatory mechanism of leukocyte and monocyte adhesion and tissue infiltration regulated by endocrine TGF-β1. (*J. Clin. Invest.* 1995. 95:2539–2554.)
Key words: TGF-β receptor • systemic TGF-β • microvasculature • inflammation • endoglin

Introduction

The families of TGF-β ligands and receptors represent a complex array of signal transducing molecules whose functional roles in vivo are under evaluation by a variety of approaches. Three mammalian isoforms of TGF-β (-β1, -β2, -β3), which in general have similar biological activities, have been identified (1). Affinity labeling experiments and cDNA cloning studies have identified three types of cell surface TGF-β receptors (1, 2). They constitute a family of receptors that includes the type III/betaglycan receptor and endoglin and a family of signaling receptors, the type I and type II receptors. The type III receptor family has been postulated to mediate delivery of ligand to a heteromeric complex and activation of type I and type II receptors (3–5). Signal transduction has been suggested to be mediated through the cytosolically exposed serine/threonine kinase domains of the type I and type II receptor heterodimer (6). Furthermore, it is known that TGF-β binds to several soluble proteins, including serum proteins and extracellular matrix–associated proteins (7).

The majority of studies on the activities of TGF-βs have been carried out in cell culture with effects observed on cell growth, differentiation, and/or extracellular matrix deposition (1, 8, 9). The actions of TGF-βs in vivo have more recently been addressed, in part by using either locally or systemically administered recombinant TGF-βs in whole animal models (10). In general, administered TGF-βs promote the repair of soft tissue, bone, and ischemic damage. They also reduce the severity of autoimmune diseases. These results are consistent with the growth-modulatory and immunosuppressive effects of TGF-βs observed in vitro, and they point to potential therapeutic applications for TGF-β.

Recently, an important role for blood-borne TGF-β1 has been inferred from studies in the MRL/1pr autoimmune mouse in which excess TGF-β in the circulation was found to compromise the immune system (11). Remarkably, delivery of maternal TGF-β pre- and postnatally to homozygous TGF-β1 gene–disrupted mice resulted in an endocrine supply of the growth factor capable of supporting embryogenesis and growth (12). Upon depletion of this maternal supply, premature death was linked to an excessive inflammatory response (13, 14).

To identify the cellular targets of endocrine TGF-β in vivo, we have used a well-established method for visualizing and quantifying hormone and growth factor binding sites after the systemic administration of ^{125}I-labeled ligands in vivo (15). The protocol involves the injection of ^{125}I-labeled ligand into the systemic circulation, fixation of the ligand at its binding sites, and visualization of the ligand by light and electron microscope radioautography of tissue sections. This technique of in vivo injection and radioautography has been used to visualize insulin (16), prolactin (17), calcitonin (18), parathyroid hormone (19), epidermal growth factor (20, 21), atrial natriuretic factor (22), angiotensin II (23), and ACTH (24) binding to receptors on target cells in vivo. These experiments revealed previously unrecognized binding sites relevant to the physiological functions of the cognate ligands.

In the present study we have used the radioautographic technique to evaluate the distribution of ^{125}I-TGF-β1–specific binding sites that are accessible to endocrine TGF-β1, and we have defined the vascular endothelium, and especially that of the microvasculature, as a major site of TGF-β1–specific binding in vivo at 2.5 min after injection. The endothelial binding sites that we observed at this time were saturable and could be distinguished from binding sites related to clearance, i.e., the proximal convoluted tubule of the kidney for uncomplexed

Address correspondence to Dr. J. J. M. Bergeron, Department of Anatomy and Cell Biology, McGill University, 3640 University Street, Montreal, Quebec H3A 2B2, Canada. Phone: 514-398-6351; FAX: 514-398-5047. Dr. A. Philip's present address is Department of Surgery, Montreal General Hospital, Montreal, Quebec H3G 1A4, Canada.

Received for publication 6 July 1994 and in revised form 22 December 1994.

J. Clin. Invest.

0021-9738/95/06/2539/16 $2.00
Volume 95, June 1995, 2539–2554

^{125}I-TGF-β1 or the hepatocyte for ^{125}I-TGF-β1 complexed with α_2-macroglobulin–methylamine (α_2-M–MeNH$_2$).[1] Furthermore, endothelial binding sites are unlikely to be related to transit of ligand to other tissues since, even at longer times of 15, 30, 45, or 60 min after the injection of ^{125}I-TGF-β1, only endocytic events in endothelium were seen, and no other cell types in the tissues examined revealed specific binding.

Methods

Quantitative radioautography. Light microscopy (LM) and electron microscopy (EM) experiments were carried out under conditions that led to the quantitative assessment of specific binding. For LM radioautography, this included the use of emulsion (NTB2; Eastman Kodak Co., Rochester, NY), which was calibrated with ^{3}H-labeled sources for efficiency of detection (25) with plastic-embedded sections of 0.5 μm thickness. For EM radioautography, monolayer application was with the semiautomatic coating device (26) and was evaluated by EM to ensure that a monolayer was indeed applied. Sections of plastic-embedded tissues were cut for EM, and section thickness was measured by the method of Small (27).

The criteria of dose–response and saturability of binding were evaluated on the basis of injecting low doses (0.03 μg) into experimental mice (22 g body wt) and higher doses (0.8 and 1 μg) into experimental rats ($\sim$ 100±15 g body wt), with control rats receiving the same dose of ^{125}I-labeled TGF-β1 coinjected with excess unlabeled ligand (50 μg or 19.6 μg) (15).

Radioiodination, injection, and tissue processing for radioautography. Radioiodination of TGF-β1 was carried out as previously described (28). Briefly, 10 μg of recombinant TGF-β1 (from Bristol-Myers Squibb, Seattle, WA) in 5 mM HCl was diluted in 20 μl of 1.5 M sodium phosphate, pH 7.4, and iodinated with 1 mCi ^{125}I-Na by the addition of 10 μl of chloramine T (20 μg/ml in 1.5 M Na phosphate, pH 7.4) at 0, 2, and 3.5 min. After stopping the reaction after 4.5 min with 40 μl tyrosine (9 mg/ml), 400 μl KI (10 mg/ml in 50 mM sodium phosphate, pH 7.4, and 400 μl urea (1.2 g/ml in 1 M HCl), the radiolabeled ligand was chromatographed on a PD-10 column. The sp act was determined (59–146 μCi/μg) and biological activity was tested by evaluating specific binding to 3T3 cells as described by Wakefield et al. (29). Radioiodination of α_2-macroglobulin–methylamine was as described previously (28). All injections were buffered to a pH of 7.4 with phosphate buffer.

For experiments evaluating initial sites of localization, male CD1 mice (22 g) were injected with a low dose (n = 2) of ^{125}I-TGF-β1 (10 × 10^6 cpm, S.A. = 146 μCi/μg). Male Sprague-Dawley rats were injected with a higher dose (n = 2) of ^{125}I-TGF-β1 (250 × 10^6 cpm; S.A. = 140 μCi/μg). Control rats (n = 2) were coinjected with ^{125}I-TGF-β1 (250 × 10^6 cpm; SA = 140 μCi/μg) and an excess of unlabeled TGF-β1 (50 μg). After 2.5 min the rats or mice were perfused with Ringer's lactate solution until blanching of the liver occurred (20–30 s), followed by perfusion fixation for 10 min with 5% glutaraldehyde in 0.05 M sodium cacodylate buffer (pH 7.3) containing 0.05% $CaCl_2$. For experiments examining localization 15 min after injection, experimental rats (n = 2) were intravenously injected with ^{125}I-TGF-β1 (250 × 10^6 cpm; SA = 115 μCi/μg). Control rats (n = 2) were coinjected with ^{125}I-TGF-β1 (250 × 10^6 cpm; SA = 115 μCi/μg) and an excess of unlabeled TGF-β1 (50 μg). A further series of experiments was carried out in which rats were injected with 0.8 μg of ^{125}I-TGF-β1 (110 × 10^6 cpm; SA = 59 μCi/μg) and perfused with Ringer's lactate followed by fixation perfusion at 2.5, 15, 30, 45, and 60 min as described above. Control experiments were carried out for the 30-min time point with the same dose of ^{125}I-TGF-β1 injected but with excess unlabeled TGF-β1 (19.6 μg). All tissues were further fixed overnight at 4°C. Tissues were washed in 0.1 M sodium cacodylate buffer containing 0.05% $CaCl_2$, postfixed with 1% osmium tetroxide in 1.5% potassium ferrocyanide for 2 h, washed again with sodium cacodylate buffer, dehydrated in increasing gradations of acetone, infiltrated, and embedded in Epon-812 (JBEM Supplies, Montreal, Canada).

For clearance experiments, CD1 mice (n = 2) were injected with a mixture of ^{125}I-TGF-β1 (10 × 10^6 cpm; SA = 146 μCi/μg) complexed to unlabeled α_2-macroglubulin–methylamine (830 μg). In separate experiments, CD1 mice (n = 3) were injected with ^{125}I-α_2-macroglobulin–methylamine (50 × 10^6 cpm; SA = 3.3 μCi/μg) to identify binding sites for α_2-macroglobulin. In these clearance experiments, mice were perfused with Ringer's lactate 2.5 min after injection, and tissues were processed as described above.

LM radioautography. LM sections (0.5 μm) were cut, prestained with iron alum and hematoxylin, dipped in NTB2 liquid emulsion, and exposed (25). Time of exposure varied with respect to tissues and is indicated in figure legends. Slides were developed in developer (D-19b; Eastman Kodak Co.).

EM radioautography. Sections in the range of 100 nm were cut with a diamond knife, dipped in Ilford L-4 nuclear emulsion Ilford Canada, Markham, Ontario and processed for EM radioautography (30). After exposure times indicated in figure legends, the sections were developed in either D-19b or Agfa-Gevaert developer for filamentous or fine grain visualization, respectively (31). Tissue sections were then treated with either glacial acetic acid for 5–15 s or amyl acetate for 30–60 s to remove the celloidin coat, stained with uranyl acetate and lead citrate for 5 and 2 min, respectively, and examined with an electron microscope (2000FX, JEOL USA Inc., Peabody, MA).

Quantitation. For LM radioautography, silver grains were counted using a micrometer ocular grid (Bausch & Lomb, Inc., Rochester, NY) at a magnification of 1,000. The grid consisted of 6 × 6 frames, each frame having the dimension of 17 μm × 17 μm. Grain counts from experimental animals were compared to grain counts from control animals (i.e., plus excess unlabeled TGF-β1), and percent competition was evaluated.

For EM radioautography, filamentous grain concentrations in experimental and control tissues were evaluated for percent competition. Shared grains were attributed to either cell type using the method described by Nadler (32).

Endothelial cell labeling was seen in all organs and tissues. Hence, to quantify the number of binding sites over endothelial cells at 2.5 min after injection of ^{125}I-TGF-β1, the method described by Fertuck and Salpeter (33) and Bergeron et al. (34) was used. Briefly, the analysis was carried out on a total of 181 photomicrographs taken wherever radioautographic grains were visualized. Taking into account the decay of ^{125}I-TGF-β1 from the time of injection, the duration of exposure, and the half-life of ^{125}I, the number of grains over endothelial cells in the various tissues was normalized (see Table V). The surface area of the endothelium under analysis was then measured. The perimeter of the endothelial plasma membrane was measured with an optical planimeter (MOP-3, Carl Zeiss, Inc., Thornwood, NY) correcting for magnification differences. Section thickness was determined by the fold method of Small (27) and found to be 112±8 nm (n = 10), and surface area was thereby calculated. Using the value of 60% efficiency of detection of ^{125}I sources with monolayer Ilford L-4 emulsion (35), the grain density (normalized number of grains/square micrometer of plasma membrane) over endothelial cells was calculated.

Results

^{125}I-TGF-β1 binding in kidney. Kidney was evaluated as a potential target because of the demonstration that antibodies to TGF-β1 reverse glomerulonephritis (36–38) as well as the observation that kidney is a major site of accumulation of TGF-β1 in vivo (39). Binding was demonstrated in kidney glomeruli of mice (Fig. 1 *a*) and rats (Fig. 1, *b* and *c*). Both kidney glomeruli (Fig. 1, *a* and *b*) as well as the epithelium of the

1. *Abbreviations used in this paper:* α_2-M–MeNH$_2$, α_2-macroglobulin–methylamine complex; EM, electron microscopy; LM, light microscopy; SA, specific activity.

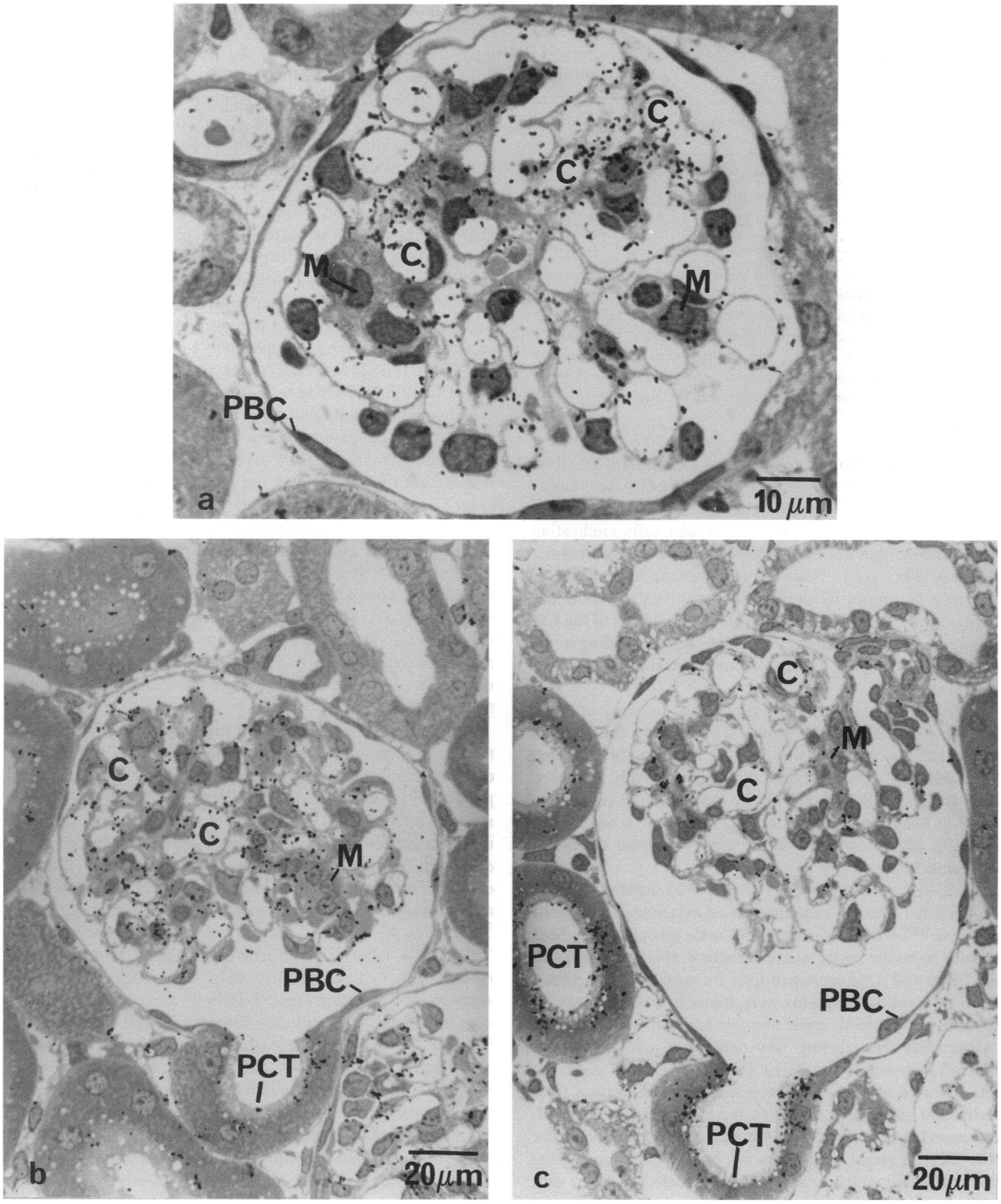

Figure 1. LM radioautographs showing the distribution of silver grains over the kidney glomerulus 2.5 min after the injection of (*a*) low doses (10×10^6 cpm), and (*b*) higher doses (250×10^6 cpm) of ^{125}I-TGF-β1 in mouse and rat, respectively. Silver grains are found over glomerular capillaries (*C*). Mesangial cells (*M*) are overlaid by fewer grains. The parietal layer of Bowman's capsule (*PBC*) shows only low labeling. In *b*, the luminal surface of the proximal convoluted tubule (*PCT*), seen emanating from the urinary pole of the renal corpuscle, shows labeling. In control rats (*c*) injected with the same amount of radiolabeled ^{125}I-TGF-β1 (250×10^6 cpm) but coinjected with excess unlabeled TGF-β1 (50 μg), diminished labeling is seen over the capillaries (*C*) in the glomerular tufts. However, high labeling is seen over the apex of the proximal convoluted tubule (*PCT*) at the urinary pole of the renal corpuscle. Exposure: *a*, 60 d; *b* and *c*, 2 d.

Table I. LM Radioautography of ^{125}I-TGF-β1 Binding Sites in Kidney

	Kidney glomerulus		Proximal convoluted tubule	
	Number of grains	Grains/289 μm²	Number of grains	Grains/289 μm²
Experimental	3,053	30.9±3.5	468	6.1±1.6
Control	584	7.1±1.4	299	5.1±0.2
Percent competition	—	77.0	—	16.4

Tissues were processed as described in Methods, and silver grains were counted over kidney glomeruli and proximal convoluted tubules from sections of either experimental rats injected with ^{125}I-TGF-β1 (250×10^6 cpm) or control rats coinjected with ^{125}I-TGF-β1 (250×10^6 cpm) and excess unlabeled TGF-β1 (50 μg). The results (grains per 17 μm × 17 μm frame) are the mean for each animal± ½ variation of two experimental and two control rats. The exposure was for 2 d.

proximal convoluted tubule (Fig. 1 *b*) were overlaid by silver grains. However, when specificity was evaluated by the coinjection of ^{125}I-TGF-β1 and excess unlabeled TGF-β1, radiolabeling was greatly diminished over glomerular tufts (indicating specific binding) but not over the proximal convoluted tubular epithelium (Fig. 1 *c*). Non–receptor-mediated clearance of polypeptide hormones by the proximal convoluted tubule has been previously demonstrated (17, 40). Quantitation of the LM radioautographic observations confirmed that the binding to the glomeruli but not to the proximal convoluted tubules was specific (Table I).

As assessed by EM radioautography, the majority of silver grains were localized to the glomerular capillary endothelium and adjacent podocytes of the glomerular tuft (Fig. 2, *a* and *b*). This labeling was specific since it was efficiently competed by excess unlabeled TGF-β1 (Table II). The low percentage of labeling found over mesangial cells (cf Fig. 2, *b* and *c*) was nonspecific since it was not appreciably competed by excess unlabeled TGF-β1 (Table II).

^{125}I-TGF-β1 binding in liver. Since Wakefield et al. (41) have identified sites of accumulation of systemically administered active ^{125}I-TGF-β1 in liver, and since this organ has been postulated to be the major site of clearance of circulating TGF-β1 in the rat (42), we examined liver for specific binding sites. At the LM level, silver grains were found over liver sinusoids in sections from experimental animals injected with ^{125}I-TGF-β1 alone, and this labeling was reduced in control animals coinjected with excess unlabeled TGF-β1 (Fig. 3, *a* and *b*).

As assessed by EM radioautography of liver sections from experimental rats (Fig. 3, *c* and *d*), the majority of silver grains were located over the endothelium and adjacent luminal space (Table III). A small percentage of grains were found over sinusoidal lining cells, mainly Kupffer cells and Ito cells (16.7%; Table III). Hepatocyte labeling was largely restricted to the sinusoidal surface and accounted for 31.8% of the grains, including those over Disse's space, where hepatocyte microvillus processes are found. In sections from control animals, silver grains over both endothelium and hepatocytes were markedly reduced (Table III). Although liver parenchyma did reveal specific binding sites confirming the conclusions of Wakefield et al. (41) and Coffey et al. (42), the majority of specific binding was not to liver parenchyma but to sinusoidal endothelium.

Effect of α_2-M–MeNH$_2$ on ^{125}I-TGF-β1 binding in kidney and liver. α_2-M is an abundant serum protein that is able to interact with TGF-β1 and affect its receptor binding and biological activities (43). It has been postulated that TGF-β1, when it is complexed with α_2-M–MeNH$_2$, is cleared from the circulation by the α2-M receptor on hepatocytes (28, 44). Accordingly, we compared the distribution in mouse kidney and liver sections of ^{125}I-TGF-β1 to that of ^{125}I-α_2-M–MeNH$_2$ and the ^{125}I-TGF-β1/α_2-M–MeNH$_2$ complex. As seen in Fig. 4 *a*, binding of ^{125}I-TGF-β1 alone was over kidney glomerulus and the proximal convoluted tubule (as seen in Fig. 1). When the ^{125}I-TGF-β1 was preincubated with an excess of unlabeled α_2-M-MeNH$_2$ to form the ^{125}I-TGF-β1/α_2-M–MeNH$_2$ complex, a diminishment of labeling over the glomerular tuft was observed (Fig. 4 *b*), while complete absence of labeling over the proximal convoluted tubule was evident (Fig. 4 *b*). The reduction in binding over the glomerular tuft is likely due to the fact that α_2-M is able, under these conditions (i.e., activated with MeNH$_2$), to complex with ^{125}I-TGF-β1 and prevent its binding to cell surface receptors (43). The lack of binding to the proximal convoluted tubule is likely due to the inability of the high molecular weight ^{125}I-TGF-β1/α_2-M–MeNH$_2$ complex (molecular mass > 700 kD) to penetrate the glomerular basement membrane.

An examination (Fig. 4 *c*) of mouse liver sections showed that the injection of ^{125}I-TGF-β1 alone resulted in a distribution of silver grains that were predominantly endothelial (sinusoidal periphery) (as in Fig. 3). The injection of ^{125}I-α_2-M–MeNH$_2$ revealed a silver grain distribution that was distinctly different, in that a greater proportion of silver grains were over hepatocytes (Fig. 4 *d*, *arrows*). This is consistent with the clearance of α_2-M–MeNH$_2$ from the circulation through the hepatocyte-restricted α2-macroglobulin receptor (28). Injection of the ^{125}I-TGF-β1/α_2-M–MeNH$_2$ complex led to a redistribution of the ^{125}I-TGF-β1 label from primarily endothelial (sinusoidal periphery, Fig. 4 *c*) to hepatocyte (Fig. 4 *e*). These observations support our conclusion that ^{125}I-TGF-β1 alone binds to specific sites in endothelium, and they demonstrate that the binding of ^{125}I-TGF-β1 could be altered by the formation of a complex between ^{125}I-TGF-β1 and α_2-M–MeNH$_2$; i.e., ^{125}I-TGF-β1 was redirected from the endothelium to the α_2-macroglobulin receptor of hepatocytes.

Lung. The lung was examined since it is a highly vascular organ (45). After the injection of ^{125}I-TGF-β1 alone, LM radioautography showed high concentrations of silver grains over alveolar walls in sections from experimental animals (Fig. 5

Figure 2. EM radioautographs showing the localization of ^{125}I-TGF-β1 binding sites 2.5 min after either injection of ^{125}I-TGF-β1 alone (250×10^6 cpm) (*a*, *b*) or with coinjection of ^{125}I-TGF-β1 (250×10^6 cpm) and excess unlabeled TGF-β1 (50 μg) (*c*) in rat kidney glomeruli. In *a*, filamentous silver grains are found mainly over capillary endothelium (*En*) and podocyte foot processes (*fp*). The cell body of the podocyte (*Podo*) is overlaid by few silver grains. In *b*, mesangial cells (*M*) show lower labeling in comparison to the adjacent capillary endothelial cells (*En*). In *c*, taken from a control rat, labeling over capillary endothelium (*En*) is diminished while that over mesangial cells (*M*) remains high. Exposure: *a*, 165 d; *b* and *c*, 26 d.

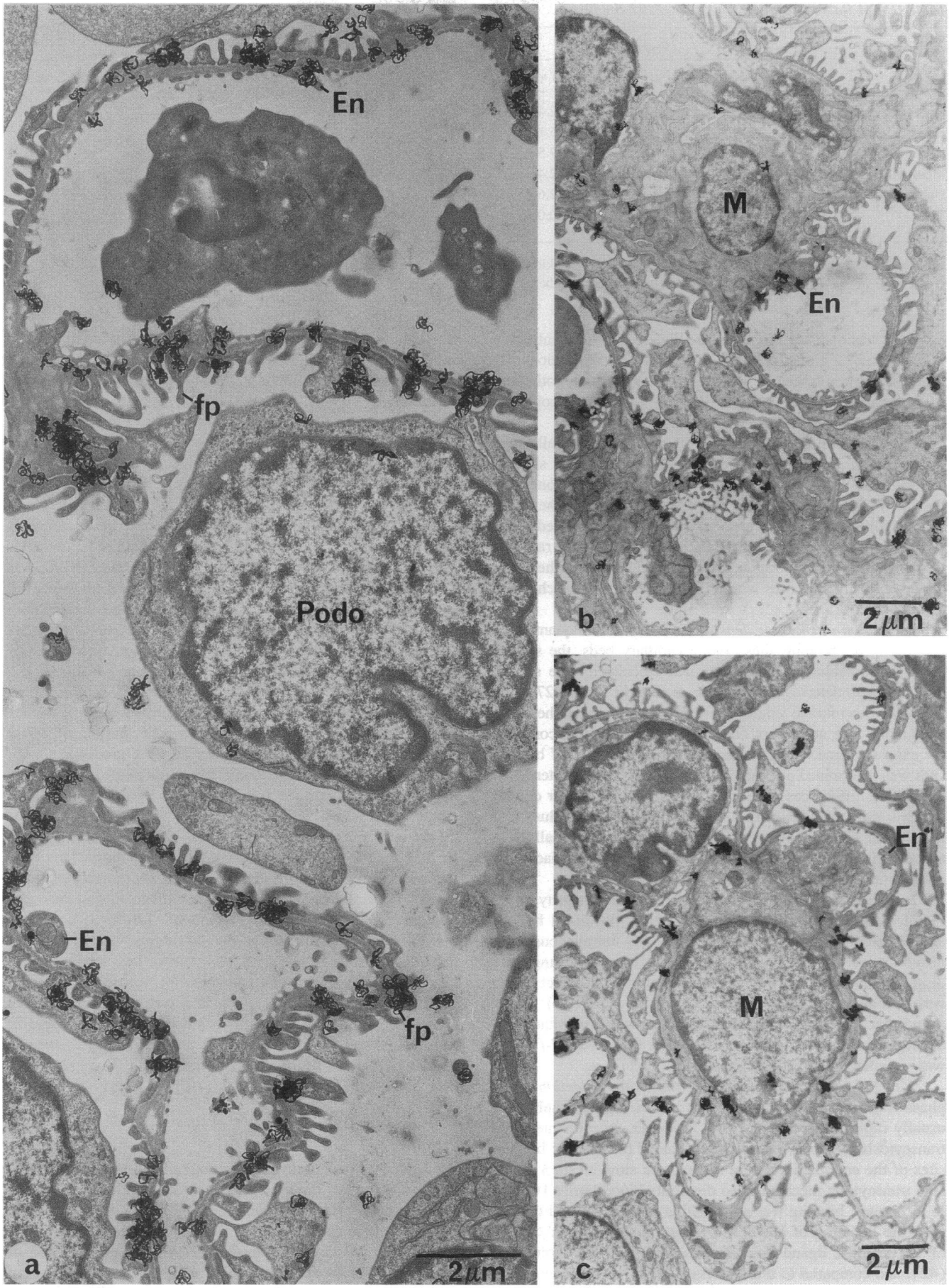
En
fp
Podo
En
fp
2 μm
a
M
En
2 μm
b
En
M
2 μm
c

Table II. EM Radioautography of ^{125}I-TGF-β1 Binding Sites in Kidney Glomeruli

	Experimental		Control		Percent competition
	Number of grains	Percentage of total grains	Number of grains	Percentage of total grains	
Podocyte	146	32.4	69	37.9	52.7
Basal lamina	68	15.1	25	13.7	63.2
Endothelial cell	124	27.5	17	9.4	86.3
Mesangial cell	56	12.4	49	26.9	12.5
Unascribed	57	12.6	22	12.1	61.4
Total	451	100.0	182	100.0	59.6

Distribution of silver grains over EM radioautographs of rat kidney glomeruli 2.5 min after injection of either ^{125}I-TGF-β1 (250 × 10^6 cpm) or coinjection of ^{125}I-TGF-β1 (250 × 10^6 cpm) and excess unlabeled TGF-β1 (50 μg).

a). This was displaced in controls (Fig. 5 *b*), and quantitation indicated a 77.2% displacement (Table IV). By EM radioautography, silver grains were found over the continuous endothelium of lung capillaries but not over adjacent alveolar macrophages nor type I or type II pneumocytes (Fig. 5 *c* and *d*).

Other soft tissues. LM radioautography of the small intestine, cerebral cortex, and cardiac and skeletal muscle showed silver grains 2.5 min after injection of ^{125}I-TGF-β1 alone over the microvasculature as well as the endothelium of the aorta. This labeling was specific since coinjection of unlabeled TGF-β1 led to lower labeling in all cases (Table IV). By EM radioautography (Fig. 6), silver grains were found only over the endothelial cells of capillaries within the parenchyma of each organ examined.

Estimation of receptor density. To compare the quantitative distribution of binding sites among capillary beds, the surface area of endothelial plasmalemma was calculated. The section thickness was determined using the method of Small (27), and the plasma membrane length was measured directly on the radioautographs. The number of observed silver grains was corrected for exposure time, and an estimation of the density of binding sites was determined as described by Fertuck and Salpeter (35). Significant differences were found, with 3.2-fold higher density of silver grains for the endothelium of kidney glomerulus, liver than for the endothelium of tibia, enamel organ, and small intestine, which in turn was 2.4-fold higher than that of cardiac, lung, aortic, and cerebral endothelium (Table V).

Integrity of ^{125}I-TGF-β1 in vivo. To test the integrity of the radioiodinated ^{125}I-TGF-β1 that was being visualized by LM and EM radioautography, ^{125}I-TGF-β1 was intravenously injected into rats (n = 2), and kidney, liver, heart, and lung were dissected and homogenized at 4°C. The amount of intact ligand was then evaluated by precipitation with 5% TCA (20). It was found that > 90% of radiolabeled ligand was precipitated for all organs examined, demonstrating that the ^{125}I-TGF-β1 that was visualized was indeed intact (Table VI).

^{125}I-TGF-β1 distribution at later times after injection. Fluid phase transport of macromolecules across the endothelium is usually rapid, i.e., seconds (46). However, receptor-mediated transcytosis may be slower. To evaluate if the specific binding sites of the endothelium were related to a slow receptor-mediated transcytotic mechanism to distribute blood-borne TGF-β1 to local sites, binding was evaluated at 15, 30, 45, and 60 min after the injection of ^{125}I-TGF-β1, i.e., at times when > 80% of the injected ligand has been cleared from the circulation (42), and compared to that observed at 2.5 min after injection. No new cell types or structures, such as connective tissue or extracellular matrices, were radiolabeled at any of the time intervals examined. For all tissues examined, i.e., kidney, liver, small intestine, and lung tissues, silver grains remained over the endothelium.

As illustrated for the kidney glomerulus (Fig. 7), light microscope radioautography of tissue sections revealed silver grains over the glomerular tuft for up to 60 min after injection of a single bolus of ^{125}I-TGF-β1. Control experiments at 30 min after injection, where excess unlabeled TGF-β1 was coinjected, revealed a marked diminution in silver grains over the glomerular tufts (cf Fig. 7, *c* and *f*). This was also seen at 15 min after injection for control experiments in which excess TGF-β1 was coinjected (data not shown). Hence, at 2.5 min as well as at later time points, the distribution of silver grains over endothelial targets was specific. By contrast, the density of silver grains over the proximal convoluted tubule was not diminished by coinjection of excess TGF-β1 and sampling at 2.5 min (Fig. 1 *c*), 15 min (not shown), and 30 min (Fig. 7 *f*), demonstrating the nonspecific nature of the binding sites at all time points. Additionally, the clearly intracellular distribution of silver grains seen at 30 min after injection over the proximal convoluted tubule was indicative of internalization of the label initially bound at the cell surface at 2.5 min after injection (cf Figs. 1, *c* and 7 *f*).

At later time points, no new cell types exhibited specific binding for ^{125}I-TGF-β1. However, the distribution of the label at the electron microscope level at 15 min after injection clearly indicated internalization into endocytic components of the endothelium (Fig. 8). Remarkably, although ^{125}I-TGF-β1 was internalized into endothelium by a specific receptor-mediated mechanism at the later time points, this did not lead to the marked loss of radiolabel from the endothelium even at 60 min after injection (cf Fig. 7, *a* and *e*). This is in contrast to the proximal convoluted tubule, where internalization via nonspecific binding sites led to the loss of radiolabel, presumably by lysosomal degradation at 30–45 min after injection.

Discussion

We have used quantitative radioautography to visualize specific binding sites after the systemic administration of recombinant active ^{125}I-TGF-β1. Vascular endothelium was revealed as the major cell type exhibiting specific binding sites. Tissue-bound ^{125}I-TGF-β1 was intact as evaluated by TCA precipitation of extracted radiolabeled ligand. The binding to the endothelium was characteristic of a high-affinity receptor-mediated interac-

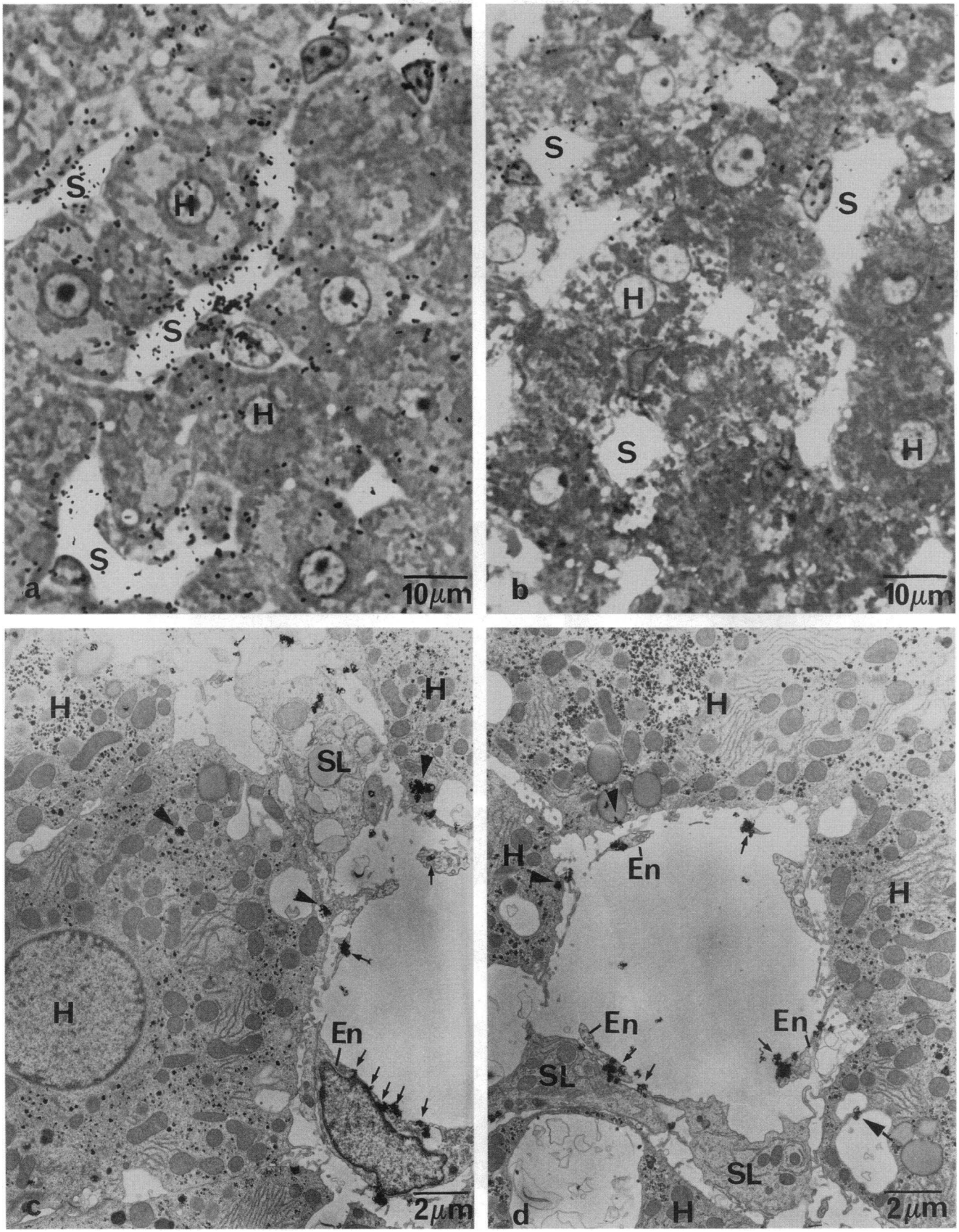

Figure 3. LM and EM radioautographs of ^{125}I-TGF-β1 binding sites in liver 2.5 min after injection of ^{125}I-TGF-β1 alone (250×10^6 cpm) (*a, c, d*), or along with excess unlabeled TGF-β1 (50 μg) (*b*). In the liver of experimental rats (*a, c, d*), silver grains (*c* and *d, arrows*) are concentrated over the sinusoidal endothelium (*S* in *a; En* in *c* and *d*). Hepatocytes also show specific labeling (*H*) (*c* and *d, arrowheads*). In control tissues (*b*), far fewer grains are found over liver sinusoids (*S*). *SL*, sinusoidal lining cell. Exposure: 3 d for *a* and *b*; 165 d for *c* and *d*.

Table III. EM Radioautography of ^{125}I-TGF-β1 Binding Sites in Liver

	Experimental		Control		Percent competition
	Number of grains	Percentage of total grains	Number of grains	Percentage of total grains	
Endothelium	228	50.1	100	55.2	56.1
Hepatocyte and Disse's space*	145	31.8	73	40.4	49.7
Other lining cells‡	76	16.7	6	3.3	92.1
Unascribed	6	1.3	2	1.1	66.7
Total	455	100	181	100	60.2

Distribution of silver grains over liver sections of experimental and control rats. Conditions for Table III as described in Methods. * Grains over hepatocytes were found mainly over the sinusoidal surface in Disse's space. ‡ The category sinusoidal lining cells includes Kupffer cells and Ito cells, with the majority over the former.

tion since relatively low concentrations of unlabeled TGF-β1 competed for binding.

The class of TGF-β receptor responsible for the binding observed here is unknown. However, cross-linking of ^{125}I-TGF-β1 to primary cultures of endothelial cells have revealed the type I and II TGF-β receptors (47, 48). Using the same technique together with immunoprecipitation studies using antibody to the type III receptor, we have also observed the type III receptor on primary cultures of microvascular endothelial cells (Morello, J. P., B. Mèyrick, R. Haver, M. O'Connor-McCourt. 1995. *J. Cell. Physiol.* In press.). Furthermore, endoglin (49), a prominent endothelial cell surface molecule, binds TGF-β1 with high affinity and specificity and is found as a heteromeric complex with the type I and II TGF-β signaling receptors (50).

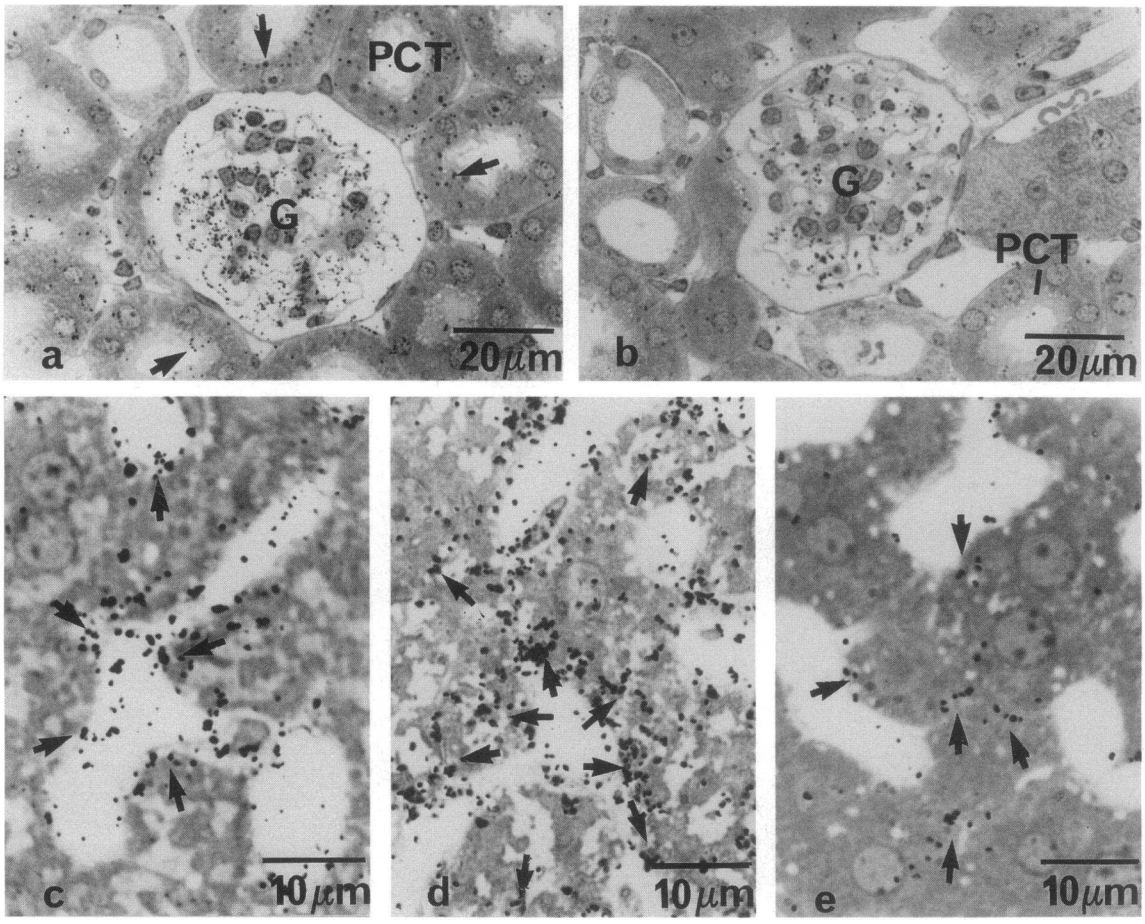

Figure 4. LM radioautographs of mouse kidney (*a, b*) and liver (*c, d, e*) at 2.5 min after the injection of ^{125}I-TGF-β1 (10×10^6 cpm) (*a, c*), [^{125}I] α_2-M–MeNH$_2$ (50×10^6 cpm) (*d*), or ^{125}I-TGF-β1 (10×10^6 cpm) complexed with excess unlabeled α_2-M–MeNH$_2$ (830 μg) (*b, e*). For ^{125}I-TGF-β1 alone, silver grains are revealed over the glomerular tuft (*G*) and proximal convoluted tubule (*PCT, arrow*) in *a*. Silver grains are diminished over the glomerular tuft (*G*) and absent from the proximal convoluted tubule in *b* when ^{125}I-TGF-β1 is complexed to α_2-M–MeNH$_2$ before injection. In *c*, the injection of ^{125}I-TGF-β1 alone reveals silver grains over the sinusoidal periphery (*arrows*). In *d*, silver grains reveal ^{125}I-α_2-M–MeNH$_2$ binding sites mainly over hepatocytes (*arrows*). The injection of ^{125}I-TGF-β1 complexed to α_2-M–MeNH$_2$ shows a localization mainly to hepatocytes (*arrows*) in *e*. Exposure: 115 d for *a, b, c,* and *e*; 39 d for *d*.

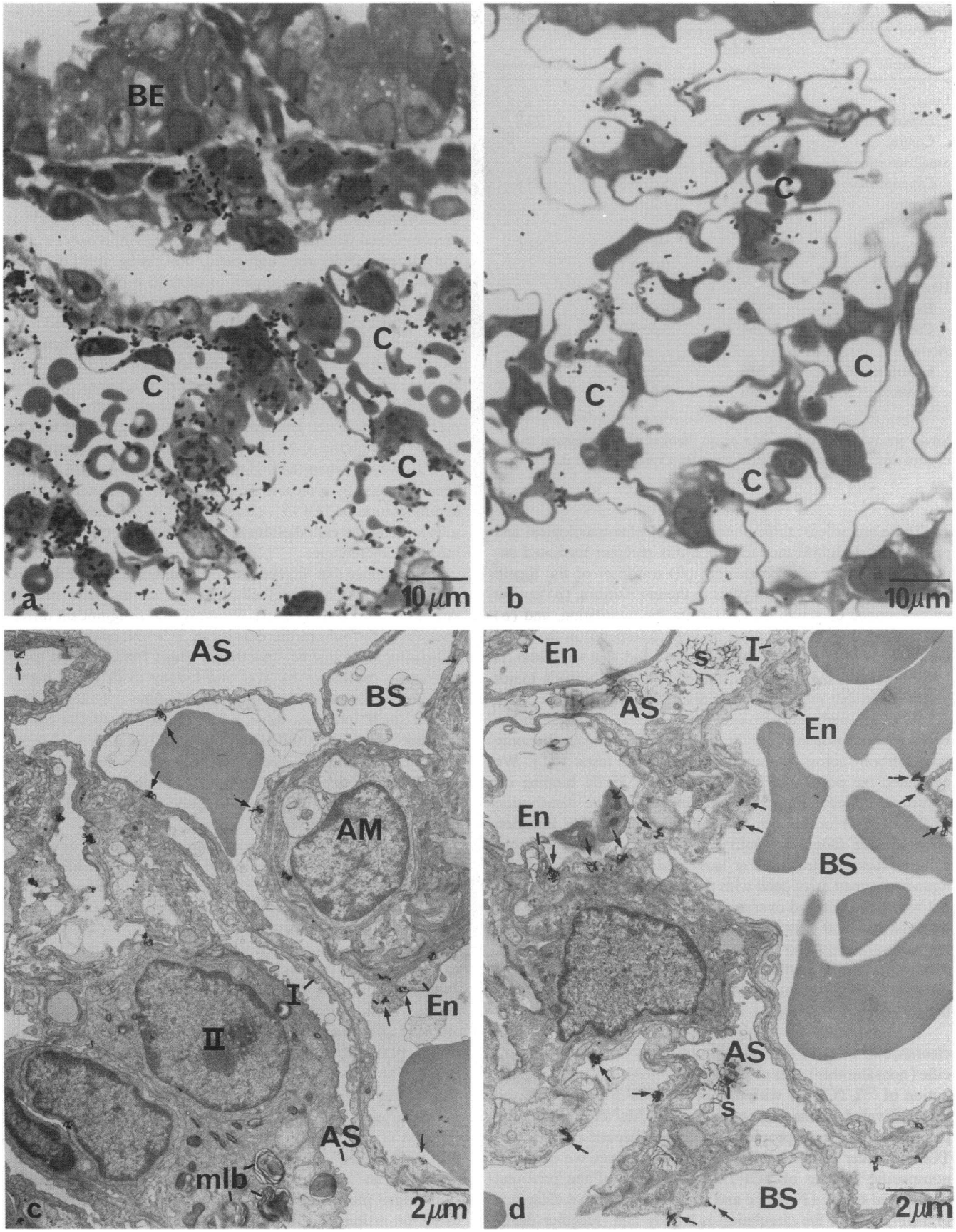

Figure 5. LM and EM radioautographs of ^{125}I-TGF-β1 binding sites in lung 2.5 min after the injection of ^{125}I-TGF-β1 alone (250 × 10^6 cpm) (*a, c, d*), or with excess unlabeled TGF-β1 (50 μg) (*b*). In the tissues of experimental rats, silver grains (*c* and *d, arrows*) are concentrated over endothelium (*En* in *c* and *d*) of lung capillaries (*C* in *a*). The bronchiolar epithelium (*BE*) is largely unlabeled. The alveoli (in all) are collapsed and the capillaries are distended because of vascular perfusion fixation conditions. No labeling is found over type I (*I*) nor type II pneumocytes (*II*). In control animals (*b*), far fewer grains are found over capillaries (*C*). *AM*, alveolar macrophage; *AS*, air space; *BS*, blood space; *s*, surfactant; *mlb*, multilamellar body. Exposure: 80 d for *a* and *b*; 7 mo for *c* and *d*.

Table IV. LM Radioautography of ^{125}I-TGF-β1 Specific Binding

Organ	Number of grains	Grain/ 89 μm²	Percent displacement
Lung			
Experimental	12,044	55.8±1.0	77.2
Control	2,732	12.7±0.8	
Small intestine			
Experimental	3,445	16.0±0.3	73.8
Control	904	4.2±0.1	
Brain			
Experimental	822	3.8±0.2	81.6
Control	138	0.7±0.1	
Heart			
Experimental	3,139	14.6±0.2	75.3
Control	764	3.6±0.9	
Aorta			
Experimental	516	2.5±0.2	68.0
Control	170	0.8±0.1	

Silver grains were counted over organ sections of experimental and control rats as described in Methods at an exposure of 80 d.

There are at least three phenomena of pharmacological and physiological significance to which this receptor-mediated endothelial binding may be related: (*a*) transport of the ligand across the endothelium to tissues in the interstitium, (*b*) uptake and clearance of active TGF-β1 from the circulation, and (*c*) receptor binding that initiates a biological response in the endothelial cells. We suggest that our data and that of others is consistent with the latter, i.e., the endothelium being a major target tissue that responds to circulating active TGF-β1.

Receptor-mediated transcytosis across the endothelium has been recently proposed for the movement of human chorionic gonadotropin across the endothelium of the testis (51). We evaluated the possibility that endothelial TGF-β1 binding involved endothelial transcytosis by examining the distribution of ^{125}I-TGF-β1 at 2.5, 15, 30, 45, and 60 min after injection (Fig. 7). We failed to identify any specific labeling of other cells, tissues, or structures at later time intervals. Indeed, the ligand remained associated with the microvascular endothelium but was now observed over endocytic components (Figs. 7 and 8) consistent with receptor-mediated ligand internalization but not receptor-mediated transcytosis across the endothelium. Analogous in vivo studies with EGF in target liver parenchymal cells have revealed that internalization is linked to a prolongation of receptor association and signal transduction (52).

We evaluated the relationship of endothelial binding to clearance of TGF-β1 from the circulation by examining nonspecific (nonsaturable) sites of uptake, and by comparing the distribution of ^{125}I-TGF-β1 with that of ^{125}I-TGF-β1 precomplexed with activated α_2-macroglobulin (α_2-M–MeNH$_2$), a binding protein that has been proposed to mediate hepatic clearance of TGF-β1 under certain conditions (28, 44). Since we observed nonspecific binding of TGF-β1 at the apex of the proximal convoluted tubule (Figs. 1 *c* and 7), we propose that clearance of TGF-β1 from the circulation is largely non–receptor mediated and is due to uptake by the proximal convoluted tubule epithelium. This was observed to be the case for all the other small peptide ligands that our laboratory and others have assessed, i.e., insulin, prolactin, calcitonin, PTH, and EGF (the molecular mass exclusion limit for basement membrane filtration is ~ 70 kD). A nonsaturable, non–receptor-mediated clearance mechanism for TGF-β1 from the circulation is also supported by our studies, which show that the kinetics and extent of clearance of ^{125}I-TGF-β1 are relatively unaffected by the coinjection of high concentrations of unlabeled TGF-β1 (unpublished observations).

The radioautographic method used here enabled us to distinguish the clearance mediated by the proximal convoluted tubule (nonspecific) from that of endothelium (specific) and that mediated by the α_2-macroglobulin receptor. When ^{125}I-TGF-β1 was precomplexed with α_2-M–MeNH$_2$, localization in the proximal convoluted tubule was abrogated, indicating that transport across the glomerular basement membrane was eliminated because of the high molecular weight of the complex (> 700,000). Also, ^{125}I-TGF-β1 radiolabeling was shifted from an endothelial to a hepatic location, confirming that the complex interacts with the α_2-M receptor on hepatocytes (28, 43, 44). Hence, it appears that under certain conditions such as wounding, where both TGF-β1 and protease-activated α_2-M are present, the TGF-β1 protease-activated α_2-M complex will be cleared through the α_2-M receptor, as previously proposed (28, 44). However, when the endogenous circulating α_2-M has not been activated by proteases as would be the case after systemic administration of TGF-β1, circulating TGF-β1 is able either to interact with the endothelium or to pass through the glomerular basement membrane.

We propose that the endothelial binding we have visualized is indicative of the endothelium being an important cellular target for endocrine TGF-β1. We observed a significant difference (~ eightfold) in the density of TGF-β1 binding sites in morphologically distinct endothelial beds (Table V). The more permeable capillaries of liver and kidney displayed a higher receptor density than the less permeable fenestrated capillaries of the small intestine, bone, and enamel organ. The lowest receptor density was found in continuous capillaries of heart, lung, aorta, and brain. The observation that TGF-β1 receptor density correlates with the three different morphological categories of endothelium suggests that these specific binding sites may be related to endothelial function.

In vitro and in vivo studies suggest that TGF-β1 is significantly involved in several aspects of endothelial cell differentiation and function. Observed responses of endothelial cell behavior include growth inhibition and induction of tubelike structures (53–56), stimulation of angiogenesis (57), induction of endothelin expression (58), a decrease in the surface density of fenestrae (59), and an inhibition of the adhesiveness of endothelial cells for neutrophils and T lymphocytes (60–62) due to a decreased synthesis of endothelial E-selectin (63). The effect of systemic TGF-β1 on the endothelium in vivo is less well understood. However, several recent studies of systemically administered TGF-β1 in whole animal models point to the endothelium as a major cellular target for circulating TGF-β1 and suggest that a major response is the reduction in adhesiveness of the endothelium for inflammatory cells. For example, TGF-β1 has been observed to exert a significant protective effect against "reperfusion injury" in several ischemic reperfusion animal models (64–66). The key mechanism is proposed to be the action of TGF-β1 on endothelial cells that prevents the adherence of polymorphonuclear leukocytes (67, 68). Furthermore, it has recently been shown that administration of TGF-β1 or TGF-β2 inhibits cerebrovascular changes and brain edema in the early phase of experimental pneumococcal menin-

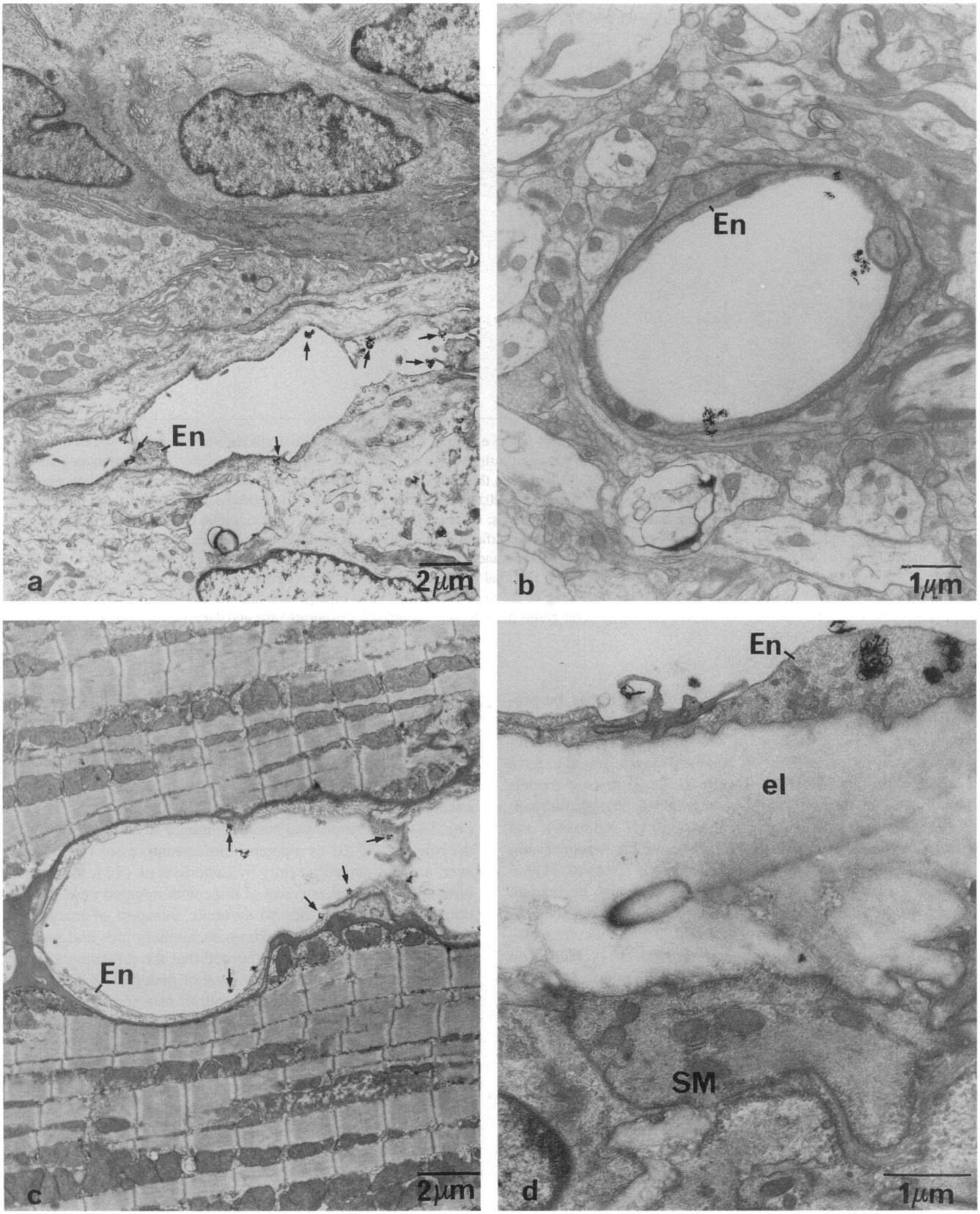

Figure 6. EM radioautographic localization of ^{125}I-TGF-β1 binding sites in (*a*) the lamina propria of the small intestinal villus, (*b*) cerebral cortex, (*c*) heart, and (*d*) aorta 2.5 min after injection of ^{125}I-TGF-β1 alone (250×10^6 cpm). Silver grains (*a* and *c*, *arrows*) are found over the endothelium (*En*) in all cases. *SM*, smooth muscle; *el*, elastic lamina. Exposure: 210 d.

Table V. Relative Grain Densities over Endothelium in Vessels of TGF-β1 Target Organs

Tissue	Endothelial type*	Plasma membrane length‡	Total number of grains§	Percent decay radioactivity‖	Normalized number of grains/μm^2¶
		μm			
Liver sinusoids	D	250	127	72	10.7
Kidney glomerulus	Fd^-	192	96	72	10.5
Tibia (vascular invasion zone)	F	1,224	111	36	3.9
Enamel organ (in papillary layer of maturation zone)	F	1,037	109	46	3.4
Small intestine (lamina propria)	F	1,517	166	67	2.6
Heart	C	1,671	138	67	1.9
Lung	C	1,717	106	69	1.4
Aorta	C	2,008	126	67	1.4
Cerebrum	C	2,921	105	67	0.9

Silver grains overlying endothelium were normalized on the basis of the exposure time as described in Methods, and normalized grains were expressed per μm^2. The luminal surface of lung endothelium has been estimated as 946 μm^2 (45). This would correspond to 1,324 binding sites on this surface alone. Assuming an equal number on the adluminal surface, this would mean ~ 2,600 binding sites per cell for lung endothelium. A similar size for endothelium of the kidney glomerulus would indicate ~ 20,000 receptors per cell. * *Fd^-*, fenestrated endothelia without diaphragms; *D*, discontinuous endothelium; *F*, fenestrated endothelia with diaphragms; *C*, continuous endothelium. ‡ From a total of 181 electron micrographs, the surface area of endothelial plasmalemma was calculated from the surface length of both the luminal and adluminal surfaces multiplied by the section thickness (112±8 nm). Surface length of the plasma membrane was measured in micrometers using an optical planimeter. § Total number of grains counted over the endothelium. ‖ Percentage of the total radioactivity injected that was detected during radioautography, taking into account the radioactivity of the ^{125}I-TGF-β1 at the beginning of the exposure, the duration of exposure, and the half-life of ^{125}I. ¶ By assuming one ligand associated with one binding site, the density of silver grains per μm^2 was corrected for exposure time and the efficiency of radioautographic detection of ^{125}I Auger electrons (60%) (35).

gitis (69). Again, it was proposed that TGF-β1 may be protecting the integrity of the endothelial blood–brain barrier by modulating the adhesiveness of the endothelial cells for inflammatory cells. Also, TGF-β1 has been demonstrated to have a protective effect in several T cell–mediated disease models including Borna disease, experimental allergic encephalomyelitis (an experimental model for human multiple sclerosis), and T cell–mediated arthritis (70–73). As with the reperfusion injury and meningitis models, the protective effect of TGF-β in these T cell–mediated disease models may also be related, in part, to the inhibitory effect of TGF-β on the adhesiveness of endothelial cells for neutrophils and T lymphocytes (60–62). In light of these in vitro and in vivo effects of TGF-β on the endothelium, it has been suggested by Gamble and Vadas (60) that maintenance of the nonadhesiveness of endothelial cells is an active phenomenon mediated by circulating TGF-β1, and by Wahl (74) that systemic TGF-β1 could target endothelial cells (74), as was demonstrated in the present study.

Table VI. ^{125}I-TGF-β1 Integrity as Evaluated by Precipitation with Trichloroacetic Acid

Organ	Radioactivity cpm/mg homogenate protein	Percent TCA precipitable
	$\times 10^{-3}$	
Kidney	8.2±0.3*	98.4±0.4
Liver	17.2±0.5	99.3±0.2
Lung	5.2±0.5	97.0±0.1
Heart	1.2±0.2	92.3±1.3

* Mean±½ variation (n = 2).

Two mouse models also support the conclusion that the endothelium is a major target for circulating TGF-β in vivo. Targeted disruption of the TGF-β1 gene in mice caused an excessive inflammatory response and death 2–3 wk after birth (13, 14). This result was initially thought to be consistent with the role of TGF-β1 as a potent immunosuppressor (75). However, as documented recently by Letterio et al. (12), the normal birth and temporary survival of mice with targeted gene disruption of TGF-β1 was due to systemic transport of maternally derived TGF-β1 from heterozygous mothers pre- and postnatally. Recently, Wahl (75) proposed that the inflammation that occurs in the mice upon the removal of maternal TGF-β1 after weaning may be due to the generation of a transient gradient of TGF-β1 between internal stores and the circulation that would be chemotactic for leukocytes. Alternately, it may be that endocrine TGF-β1 acts directly on endothelial cells to maintain their nonadhesive nature (both in normal mice and in the transgenic mice receiving maternal TGF-β1) and that removal of circulating TGF-β1 results in adhesion and leukocyte migration. Indeed, although TGF-β1 gene–disrupted mice devoid of maternal TGF-β1 were embryonic lethal (12), even the major defect in heart development may be endothelial related, since (*a*) the major defect noted by Letterio et al. (12) was abnormal cardiac development with poorly formed ventricular lumina, muscle, and valves; and (*b*) Heine et al. (76) have localized TGF-β in the endocardial cushion tissue of developing heart valves of animal embryos. Since Akhurst et al. (77) have defined an association between TGF-β and endothelial-mediated endocardial cushion formation and cardiac development,

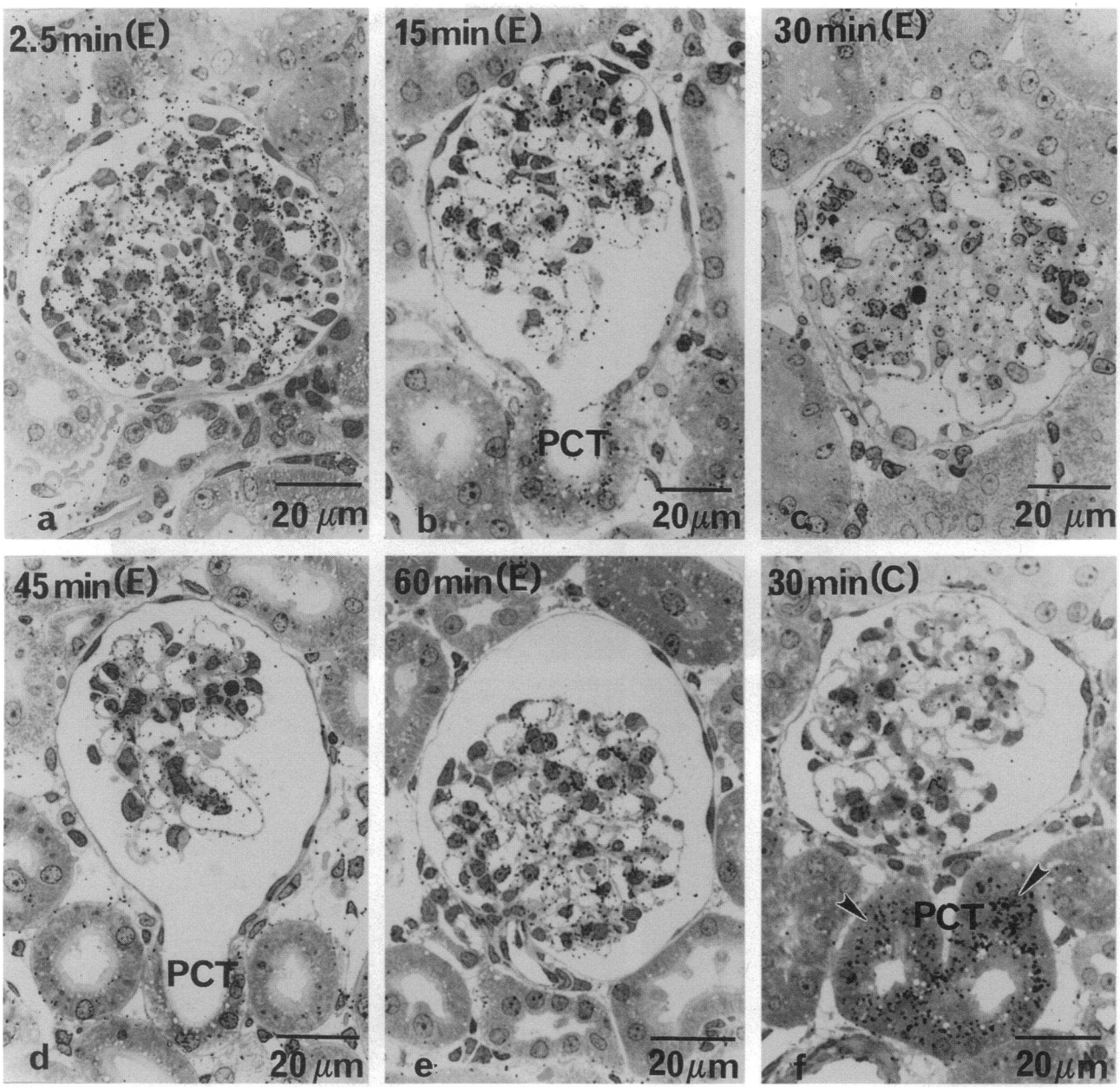

Figure 7. LM radioautographic localization of internalized ^{125}I-TGF-β1/TGF-β1 binding site complexes in kidney glomeruli at various time points after the injection of ^{125}I-TGF-β1 (110×10^6 cpm) alone (*a–e*) or after coinjection of ^{125}I-TGF-β1 (110×10^6 cpm) and unlabeled TGF-β1 (19.6 μg) (*f*). In the sections from the experimental rats (*E*), grains are seen over the kidney glomerulus 2.5 min after injection (*a*). For animals killed at 15 min (*b*), 30 min (*c*), 45 min (*d*), and 60 min (*e*), silver grains remain over the kidney glomerulus while no increase in the number of grains is found over the surrounding tissue. In control (*C*) animals (*f*) evaluated at 30 min after coinjection of ^{125}I-TGF-β1 and excess unlabeled ligand, a marked diminution in labeling over the glomerular tuft is seen. However, nonspecific binding sites in the proximal convoluted tubule are prominent in *f* and are clearly over intracellular components (*arrowheads*). Exposure: 60 d.

then even the major defect in the null homozygous TGF-β1 knockout mouse may be attributed to a defective endothelial cell differentiation. Studies with the homozygotic TGF-β1 gene–disrupted mice therefore suggest that TGF-β1 has significant roles in endothelial cell differentiation during embryogenesis and also in subsequent endothelial cell function. A second mouse model, in which the level of circulating TGF-β1 is elevated because of the expression of porcine TGF-β1 linked to the albumin enhancer/promoter, exhibits effects on endothelial cells in the kidney (78). This would be predicted from our results, which show that glomerular endothelium has the highest density of specific binding sites in vivo.

The observations discussed above define a role for circulating TGF-β1 in the preservation and stabilization of endothelial function. In contrast, other studies have directly linked increased local production of TGF-β1 to several fibrotic disorders, including hepatic cirrhosis, idiopathic pulmonary fibrosis, and glomerulonephritis (79). In these diseases it is proposed that local overproduction of active TGF-β causes the activation of fibroblasts with a resulting excessive elaboration of extracellular matrix. It appears then that circulating TGF-β1 interacts preferentially with endothelial cells, whereas locally produced and/or activated TGF-β1 may stimulate fibroblasts as proposed recently by Wahl (74). This apparent difference between the preferred cellular

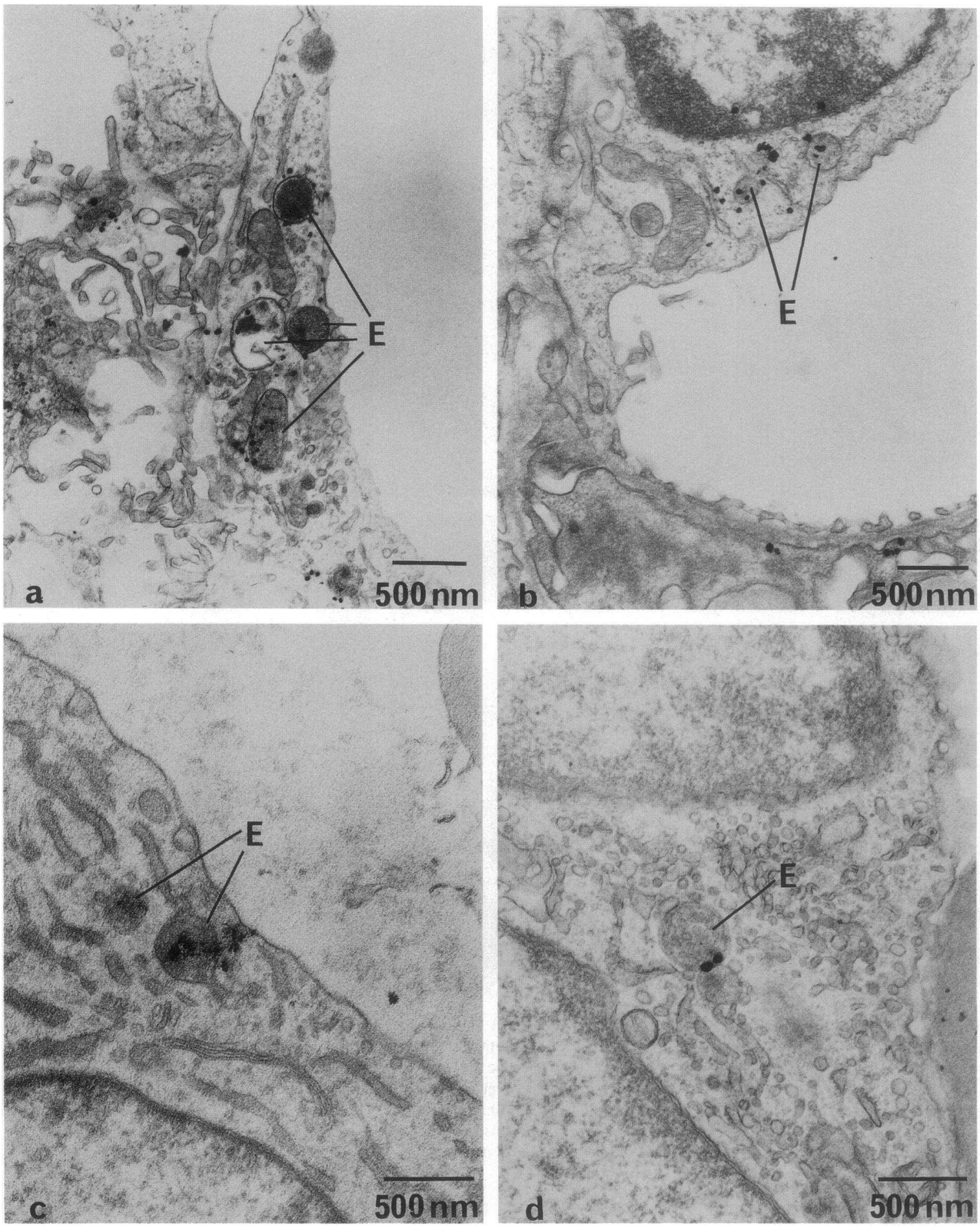

Figure 8. EM radioautographic localization of internalized ^{125}I-TGF-β1/TGF-β1 binding site complexes in distinct vascular beds 15 min after the injection of ^{125}I-TGF-β1 (250×10^6 cpm) alone. Grains are seen over components of endocytic apparatus consisting of endosomes and lysosome-like structures as well as multivesicular bodies in endothelium of liver (*a*, discontinuous endothelium); kidney (*b*, fenestrated endothelium without diaphragms); bone (*c*, fenestrated endothelium with diaphragms); and lung (*d*, continuous endothelium). Exposure: *a* and *b*, 93 d; *c*, 168 d; *d*, 188 d.

targets for circulating versus local TGF-β1 emphasizes the contextual nature of TGF-β1 action and suggests that cellular responsiveness is defined not only by the presence of cell surface receptors but also by the route of delivery.

However, circulating TGF-β1 is probably not directed exclusively to endothelial cells. It may also interact with macrophages and fibroblasts directly, as indicated by the ability of a single injection of TGF-β1 to enhance wound healing (80, 81)

and the correlation between elevated plasma TGF-β1 levels and fibrosis (82, 83). The lack of detection of ^{125}I-TGF-β1 specific binding sites in fibroblasts in the present study may be due to the low doses of ^{125}I-TGF-β1 used, or because the number of TGF-β receptors in fibroblasts is too low to be detected by the radioautographic technique. Indeed, insulin receptors in fibroblasts in vivo are undetectable by the same in vivo radioautographic method (84).

Hence, the in vivo binding studies presented here have defined the microvascular endothelium as the major site that specifically binds blood-borne TGF-β1. Endothelial cells of the microvasculature are among the least mitogenically active cells in the body (85–87), as expected for a target of TGF-β1. Additionally, the finding that a human disease characterized by vascular dysplasia (hereditary hemorrhagic telangiectasia type 1) is caused by mutations in the TGF-β receptor that is highly expressed on endothelial cells (endoglin) (88) emphasizes the importance of TGF-β in endothelial function. Taken together, present and past studies indicating a critical role for the endothelium in TGF-β action are highly relevant to the design of clinical trials that use systemically administered TGF-β1. In vivo binding studies with ^{125}I-TGF-β2 and -β3 and other ligands of the TGF-β family may reveal different cellular targets for these related but distinct ligands.

Acknowledgments

This paper is dedicated to the memory of Dr. Wei H. Lai.

We thank Dr. R. Hannah, who participated in these studies. We also thank Dr. W. H. Lai for assistance and Dr. Eugene Daniels (McGill University, Montreal, Canada) for his helpful comments on the manuscript. We also acknowledge the assistance of Jeannie Mui, Matilda Cheung, and Sonia Bujold (electron microscopy, radioautography, and photography core facilities of the Department of Anatomy and Cell Biology, McGill University).

This work was supported by grants from the Medical Research Council of Canada (H. Warshawsky), the National Cancer Institute (J. J. M. Bergeron), and the NRC of Canada (M. O'Connor-McCourt). A. Philip is a recipient of a Natural Sciences and Engineering Research Council Visiting Fellowship. We thank Bristol-Meyers Squibb for the generous gift of recombinant active TGF-β1. NRC publication No. 38523.

References

1. Roberts, A. B., and M. B. Sporn. 1990. The transforming growth factor-betas. *In* Peptide Growth Factors and Their Receptors. M. B. Sporn and A. B. Roberts, editors. Springer-Verlag, Heidelberg. 419–472.

2. Massagué, J., L. Attisano, and J. L. Wrana. 1994. The TGF-β family and its composite receptors. *Trends Cell Biol.* 4:172–178.

3. López-Casillas, F., J. L. Wrana, and J. Massagué. 1993. Betaglycan presents ligand to the TGF-β signaling receptor. *Cell.* 73:1435–1444.

4. López-Cassilas, F., S. Cheifetz, J. Doody, J. L. Andres, W. S. Lane, and J. Massagué. 1991. Structure and expression of the membrane proteoglycan betaglycan, a component of the TGF-β receptor system. *Cell.* 67:785–795.

5. Wang, X.-F., H. Y. Lin, E. Ng-Eaton, J. Downward, H. F. Lodish, and R. A. Weinberg. 1991. Expression cloning and characterization of the TGF-β Type III receptor. *Cell.* 67:797–805.

6. Franzén, P., P. ten Dijke, H. Ichijo, H. Yamashita, P. Schultz, C.-H. Heldin, and K. Miyazono. 1993. Cloning of a TGFβ Type I receptor that forms a heteromeric complex with TGFβ Type II receptor. *Cell.* 75:681–692.

7. Lin, H. Y., and H. F. Lodish. 1993. Receptors for the TGF-β superfamily: multiple polypeptides and serine/threonine kinases. *Trends Cell Biol.* 3:14–19.

8. Moses, H. L., E. Y. Yang, and J. A. Pietenpol. 1990. TGF-β stimulation and inhibition of cell proliferation: new mechanistic insights. *Cell.* 63:245–247.

9. Massagué, J., S. Cheifetz, F. T. Boyd, and J. L. Andres. 1990. TGF-β receptors and TGF-β binding proteoglycans: recent progress in identifying their functional properties. *Ann. NY Acad. Sci.* 593:59–71.

10. Border, W. A., and E. Ruoslahti. 1992. Transforming growth factor-β in disease: the dark side of tissue repair. *Cell.* 90:1–7.

11. Lowrance, J. H., F. X. O'Sullivan, T. E. Caver, W. Waegell, and H. D. Gresham. 1994. Spontaneous elaboration of transforming growth factor β suppresses host defense against bacterial infection in autoimmune MRL/lpr mice. *J. Exp. Med.* 180:1693–1703.

12. Letterio, J. J., A. G. Geiser, A. B. Kulkarni, N. S. Roche, M. B. Sporn, and A. B. Roberts. 1994. Maternal rescue of transforming growth factor β1 null mice. *Science (Wash. DC).* 264:1936–1938.

13. Kulkarni, A. B., C.-G. Huh, D. Becker, A. Geiser, M. Lyght, K. C. Flanders, A. B. Roberts, M. B. Sporn, J. M. Ward, and S. Karlsson. 1993. Transforming growth factor β_1 null mutation in mice causes excessive inflammatory response and early death. *Proc. Natl. Acad. Sci. USA.* 90:770–774.

14. Shull, M. M., I. Ormsby, A. B. Kier, S. Pawlowski, R. J. Diebold, M. Yin, R. Allen, C. Sidman, G. Proetzel, D. Calvin, et al. 1992. Targeted disruption of the mouse transforming growth factor-β1 gene results in multifocal inflammatory disease. *Nature (Lond.).* 359:693–699.

15. Bergeron, J. J. M., and B. I. Posner. 1979. In vivo studies on the initial localization and fate of polypeptide hormone receptors by the technique of quantitative radioautography. *J. Histochem. Cytochem.* 27:1512–1513.

16. Bergeron, J. J. M., G. Levine, R. Sikstrom, D. O'Shaughnessy, B. Kopriwa, N. J. Nadler, and B. I. Posner. 1977. [^{125}I]labeled insulin to hepatocyte plasmalemma as visualized by electron microscope radioautography. *Proc. Natl. Acad. Sci. USA.* 74:5051–5055.

17. Bergeron, J. J. M., L. Resch, R. Rachubinski, B. A. Patel, and B. I. Posner. 1983. Effect of colchicine on internalization of prolactin in female rat liver: an in vivo radioautographic study. *J. Cell Biol.* 96:875–886.

18. Warshawsky, H., D. Goltzman, M. R. Rouleau, and J. J. M. Bergeron. 1980. Direct in vivo demonstration by radioautography of specific binding sites for calcitonin in skeletal and renal tissues of the rat. *J. Cell Biol.* 85:682–694.

19. Rouleau, M. F., J. Mitchell, and D. Goltzman. 1988. In vivo distribution of parathyroid hormone receptors in bone: evidence that a predominant osseous target cell is not the mature osteoblast. *Endocrinology.* 123:187–191.

20. Martineau-Doizé, B., W. H. Lai, H. Warshawsky, and J. J. M. Bergeron. 1988. *In vivo* demonstration of cell types in bone that harbor epidermal growth factor receptors. *Endocrinology.* 123:841–858.

21. Martineau-Doizé, B., H. Warshawsky, K. Dickson, W. H. Lai, and J. J. M. Bergeron. 1991. Localization of epidermal growth factor receptors in cells of the enamel organ of the rat incisor. *Dev. Biol.* 148:590–601.

22. Bianchi, C., J. Gutkowska, G. Thibault, R. Garcia, J. Genest, and M. Cantin. 1985. Radioautographic localization of ^{125}I-atrial natriuretic factor (ANF) in rat tissues. *Histochemistry.* 82:441–452.

23. Bianchi, C., J. Gutkowska, C. Charbonneau, M. Ballak, M. B. Anand-Srivastava, A. De Léan, J. Genest, and M. Cantin. 1986. Internalization and lysosomal association of [^{125}I]angiotensin II in norepinephrine-containing cells of the rat adrenal medulla. *Endocrinology.* 119:1873–1875.

24. Van Houten, M., M. N. Khan, R. J. Khan, and B. I. Posner. 1981. Blood-borne adrenocorticotropin binds specifically to the median eminence-arcuate region of the rat hypothalamus. *Endocrinology.* 108:2385–2387.

25. Kopriwa, B., and C. P. Leblond. 1962. Improvements in the coating technique of radioautography. *J. Histochem. Cytochem.* 10:269–284.

26. Kopriwa, B. M. 1967. A semiautomatic instrument for the radioautographic coating technique. *J. Histochem. Cytochem.* 14:923–927.

27. Small, J. V. 1968. Measurement of section thickness. *In* Proceedings of the 4th European Congress on Electron Microscopy. Vol. 1. D. S. Bocciarelli, editor. Roma Tipographia Poliglotta, Vaticana. 609 pp.

28. Philip, A., and M. D. O'Connor-McCourt. 1991. Interaction of transforming growth factor-β1 with α2-macroglobulin: role in transforming growth factor-β1 clearance. *J. Biol. Chem.* 266:22290–22296.

29. Wakefield, L. M., D. M. Smith, T. Masui, C. C. Harris, and M. B. Sporn. 1987. Distribution and modulation of the cellular receptor for transforming growth factor-beta. *J. Cell Biol.* 105:965–975.

30. Kopriwa, B. 1973. A reliable, standardized method for ultrastructural electron microscopic radioautography. *Histochemistry.* 37:1–17.

31. Kopriwa, B. M. 1975. A comparison of various procedures for fine grain development in electron microscope radioautography. *Histochemistry.* 44:201–224.

32. Nadler, N. 1979. Quantitation and resolution in electron microscope radioautography. *J. Histochem. Cytochem.* 27:1531–1533.

33. Fertuck, H. C., and M. M. Salpeter. 1976. Quantitation of junctional and extrajunctional acetylcholine receptors by electron microscope autoradiography after ^{125}I-α-bungarotoxin binding at mouse neuromuscular junctions. *J. Cell Biol.* 69:144–158.

34. Bergeron, J. J. M., R. Sikstrom, A. R. Hand, and B. I. Posner. 1979. Binding and uptake of [^{125}I]insulin into rat liver hepatocytes and endothelium: an in vivo radioautographic study. *J. Cell Biol.* 80:427–443.

35. Fertuck, H. C., and M. M. Salpeter. 1974. Sensitivity in electron microscope autoradiography for [^{125}I]. *J. Histochem. Cytochem.* 22:80–87.

36. Border, W. A., S. Okuda, L. B. Languino, M. B. Sporn, and E. Ruoslahti. 1990. Suppression of experimental glomerulonephritis by antiserum against transforming growth factor β1. *Nature (Lond.).* 346:371–374.

37. Okuda, S., L. R. Languino, E. Ruoslahti, and W. A. Border. 1990. Elevated expression of transforming growth factor-β and proteoglycan production in experimental glomerulonephritis: possible role in expansion of the mesangial extracellular matrix. *J. Clin. Invest.* 86:453–462.

38. Okuda, S., T. Nakamura, T. Yamamoto, E. Ruoslahti, and W. A. Border.

1991. Dietary protein restriction rapidly reduces transforming growth factor-β1 expression in experimental glomerulonephritis. *Proc. Natl. Acad. Sci. USA.* 88:9765–9769.

39. Roberts, A. B., M. A. Anzano, C. A. Meyers, J. Wideman, R. Blacher, Y.-C. E. Pan, S. Stein, S. R. Lehrman, J. M. Smith, L. C. Lamb, and M. B. Sporn. 1983. Purification and properties of a type β transforming growth factor from bovine kidney. *Biochemistry.* 22:5692–5698.

40. Bergeron, J. J. M., R. Rachubinski, N. Searle, D. Borts, R. Sikstrom, and B. I. Posner. 1980. Polypeptide hormone receptors in vivo: demonstration of insulin binding to adrenal gland and gastrointestinal epithelium by quantitative radioautography. *J. Histochem. Cytochem.* 28:824–835.

41. Wakefield, L. M., T. S. Winokur, R. S. Hollands, K. Christopherson, A. D. Levinson, and M. B. Sporn. 1990. Recombinant latent transforming growth factor β1 has a longer plasma half-life in rats than active transforming growth factor β1, and a different tissue distribution. *J. Clin. Invest.* 86:1976–1984.

42. Coffey, R. J., Jr., L. J. Kost, R. M. Lyons, H. L. Moses, and N. F. LaRusso. 1987. Hepatic processing of transforming growth factor β in the rat: uptake, metabolism, and biliary excretion. *J. Clin. Invest.* 80:750–757.

43. O'Connor-McCourt, M. D., and L. M. Wakefield. 1987. Latent transforming growth factor-beta in serum. A specific complex with alpha-2-macroglobulin. *J. Biol. Chem.* 262:14090–14099.

44. LaMarre, J., M. A. Hayes, G. K. Wollenberg, I. Hussaini, S. W. Hall, and S. L. Gonias. 1991. An α_2-macroglobulin receptor-dependent mechanism for the plasma clearance of transforming growth factor-β1 in mice. *J. Clin. Invest.* 87:39–44.

45. Haies, D. M., J. Gil, and E. R. Weibel. 1981. Morphometric study of rat lung cells. *Am. Rev. Respir. Dis.* 123:533–541.

46. Simionescu, M., and N. Simionescu. 1991. Endothelial Transport of Macromolecules: Transcytosis and Endocytosis. Cell Biology Reviews. Vol. 25. M. Simionescu and N. Simionescu, editors. Springer International, University of the Basque Country. 78 pp.

47. Merwin, J. R., W. Newman, L. D. Beall, A. Tucker, and J. Madri. 1991. Vascular cells respond differentially to transforming growth factors $beta_1$ and $beta_2$ in vitro. *Am. J. Pathol.* 138:37–51.

48. Hirai, R., and K. Kayi. 1992. Transforming growth factor β1-specific binding proteins on human vascular endothelial cells. *Exp. Cell Res.* 201:119–125.

49. Cheifetz, S., T. Beltón, C. Calés, S. Vera, C. Bernabeu, J. Massagué, and M. Letarte. 1992. Endoglin is a component of the TGF-β receptor system in human endothelial cells. *J. Biol. Chem.* 267:19027–19030.

50. Yamashita, H., H. Ichijo, S. Grimsby, A. Moren, P. ten Dijke, and K. Miyazono. 1994. Endoglin forms a heteromeric complex with the signaling receptors for transforming growth factor-beta. *J. Biol. Chem.* 269:1995–2001.

51. Ghinea, N., M. T. V. Hai, M.-T. Groyer-Picard, and E. Milgrom. 1994. How protein hormones reach their target cells: receptor-mediated transcytosis of hCG through endothelial cells. *J. Cell Biol.* 125:87–97.

52. DiGuglielmo, G. M., P. C. Baass, W.-J. Ou, B. I. Posner, and J. J. M. Bergeron. 1994. Compartmentalization of SHC, GRB2, mSOS and hyperphosphorylation of Raf-1 by EGF but not insulin in liver parenchyma. *EMBO (Eur. Mol. Biol. Organ.) J.* 13:4269–4277.

53. Madri, J. A., O. Kocher, J. R. Merwin, L. Bell, A. Tucker, and C. T. Basson. 1990. Interaction of vascular cells with transforming growth factor-β. *Ann. NY Acad. Sci.* 593:243–258.

54. Madri, J. A., L. Bell, and J. R. Merwin. 1992. Modulation of vascular cell behaviour by transforming growth factors β. *Mol. Reprod. Dev.* 32:121–126.

55. Pepper, M. S., J.-D. Vassalli, L. Orci, and R. Montesano. 1993. Biphasic effect of transforming growth factor-β1 on in vitro angiogenesis. *Exp. Cell Res.* 204:356–363.

56. RayChaudhury, A., and P. D'Amore. 1991. Endothelial cell regulation by transforming growth factor-β. *J. Cell. Biochem.* 47:224–229.

57. Roberts, A. B., M. B. Sporn, R. K. Assoian, J. M. Smith, N. S. Roche, L. M. Wakefield, U. I. Heine, L. A. Liotta, V. Falanga, J. H. Kehrl, and A. S. Fauci. 1986. Transforming growth factor type β: rapid induction of fibrosis and angiogenesis in vivo and stimulation of collagen formation in vitro. *Proc. Natl. Acad. Sci. USA.* 83:4167–4171.

58. Kurihara, H., M. Yoshizumi, T. Sugiyama, F. Takaku, M. Yanagisawa, T. Masaki, M. Hamaoki, H. Kato, and Y. Yazaki. 1989. Transforming growth factor-β stimulates the expression of endothelin mRNA by vascular endothelial cells. *Biochem. Biophys. Res. Commun.* 159:1435–1440.

59. Lombardi, T., R. Montesano, M. B. Furie, S. C. Silverstein, and L. Orci. 1988. In vitro modulation of endothelial fenestrae: opposing effects of retinoic acid and transforming growth factor beta. *J. Cell Sci.* 91:313–318.

60. Gamble, J. R., and M. A. Vadas. 1988. Endothelial adhesiveness for blood neutrophils is inhibited by transforming growth factor-beta 1. *Science (Wash. DC).* 242:97–99.

61. Gamble, J. R., and M. A. Vadas. 1991. Endothelial cell adhesiveness for human T-lymphocytes is inhibited by transforming growth factor-beta 1. *J. Immunol.* 148:1149–1154.

62. McCarron, A. M., L. Wang, M. K. Racke, D. E. MaFarlin, and M. Spatz. 1993. Cytokine-regulated adhesion between encephalitogenic T-lymphocytes and cerebrovascular endothelial cells. *J. Neuroimmunol.* 143:23–30.

63. Gamble, J. R., Y. Khew-Goodall, and M. A. Vadas. 1993. Transforming growth factor-beta inhibits E-selectin expression on human endothelial cells. *J. Immunol.* 150:4494–4503.

64. Armstead, W. M., R. Mirro, S. L. Zuckerman, M. Shibata, and C. W. Leffler. 1993. Transforming growth factor-β attenuates ischemia-induced alterations in cerebrovascular responses. *Am. J. Physiol.* 264:H381–H385.

65. Karasawa, A., J. P. Guo, X.-L. Ma, and A. M. Lefer. 1991. Beneficial effects of transforming growth factor-β and tissue plus plasminogen activator in splanchnic artery occlusion and reperfusion in cats. *J. Cardiovasc. Pharmacol.* 18:95–105.

66. Lefer, A. M., P. Tsao, N. Aoki, and M. A. Palladiro, Jr. 1990. Mediation of cardioprotection by transforming growth factor-β. *Science (Wash. DC).* 249:61–64.

67. Lefer, A. M. 1991. Mechanisms of the protective effects of transforming growth factor-β in reperfusion injury. *Biochem. Pharmacol.* 42:1323–1327.

68. Lefer, A. M., X.-L. Ma, A. S. Weyrich, and R. Scalia. 1993. Mechanism of the cardioprotective effect of TGF-β1 in feline myocardial ischemia and reperfusion. *Proc. Natl. Acad. Sci. USA.* 90:1018–1022.

69. Pfister, H. W., K. Frei, B. Ottnad, U. Koedel, A. Tomasz, and A. Fontana. 1992. Transforming growth factor β_2 inhibits cerebrovascular changes in brain edema formation in the tumor necrosis factor α–independent early phase of experimental pneumococcal meningitis. *J. Exp. Med.* 176:265–268.

70. Stitz, L., O. Pfanz, T. Bilzer, K. Frei, and A. Fontana. 1991. Transforming growth factor-β modulates T-cell mediated encephalitis caused by Borna disease virus. *J. Immunol.* 147:3581–3586.

71. Johns, L. D., K. C. Flanders, G. E. Ranges, and S. Sriram. 1991. Successful treatment of experimental allergic encephalomyelitis with transforming growth factor-beta 1. *J. Immunol.* 147:1792–1796.

72. Racke, M. K., S. Dhib-Jalbut, B. Cannela, P. S. Albert, C. S. Raine, and D. W. McFarlin. 1991. Prevention and treatment of chronic relapsing experimental allergic encephalomyelitis by transforming growth factor-β1. *J. Immunol.* 146:3012–3017.

73. Kuruvilla, A. P., R. Shah, G. M. Hochwald, H. D. Liggit, M. A. Palladino, and G. J. Thorbecke. 1991. Protective effect of transforming growth factor-beta 1 on experimental autoimmune diseases in mice. *Proc. Natl. Acad. Sci. USA.* 88:2918–2921.

74. Wahl, S. M. 1994. Transforming growth factor β: the good, the bad, and the ugly. *J. Exp. Med.* 180:1587–1590.

75. Wahl, S. M. 1991. The role of transforming growth factor-beta in inflammatory processes. *Immunol. Res.* 10:249–254.

76. Heine, U. I., E. F. Munoz, K. C. Flanders, L. R. Ellingsworth, H.-Y. P. Lam, N. L. Thompson, A. B. Roberts, and M. B. Sporn. 1987. Role of transforming growth factor-β in the development of the mouse embryo. *J. Cell Biol.* 105:2861–2876.

77. Akhurst, R. J., S. A. Lehnert, A. Faissner, and E. Duffie. 1990. TGF beta in murine morphogenetic processes: the early embryo and cardiogenesis. *Development (Camb.).* 108:645–656.

78. Kopp, J. B., P. Nagy, N. Sanderson, L. Wakefield, A. B. Roberts, M. B. Sporn, and S. S. Thorgeirsson. 1994. Circulating TGF-β1 and renal disease in transgenic mice. *Clin. Res.* 42:144*a*. (Abstr.)

79. Roberts, A. B., and M. B. Sporn. 1993. Physiological actions and clinical applications of transforming growth factor-β (TGF-β). *Growth Factors.* 8:1–9.

80. Mustoe, T. A., G. F. Pierce, A. Thomason, P. Gramates, M. B. Sporn, and T. F. Deuel. 1987. Accelerated healing of incisional wounds in rats induced by transforming growth factor β. *Science (Wash. DC).* 237:1333–1336.

81. Beck, L. S., L. DeGuzman, W. P. Lee, Y. Xu, M. W. Siegel, and E. P. Amento. 1993. One systemic administration of transforming growth factor-β1 reverses age- or glucocorticoid-impaired wound healing. *J. Clin. Invest.* 92:2841–2849.

82. Coimbra, T., R. Wiggins, J. W. Noh, S. Merritt, and S. H. Phan. 1991. Transforming growth factor-β production in anti-glomerular basement membrane disease in the rabbit. *Am. J. Pathol.* 138:223–234.

83. Anscher, M. S., W. P. Peters, H. Reisenbichler, W. P. Petros, and R. L. Jirtle. 1993. Transforming growth factor β as a predictor of liver and lung fibrosis after autologous bone marrow transplantation for advanced breast cancer. *N. Engl. J. Med.* 328:1592–1598.

84. Bergeron, J. J. M., R. Rachubinski, N. Searle, R. Sikstrom, D. Borts, P. Bastian, and B. I. Posner. 1980. Polypeptide hormone receptors in vivo: demonstration of insulin binding to adrenal gland and gastrointestinal epithelium by quantitative radioautography. *J. Histochem. Cytochem.* 28:824–835.

85. Engerman, R. L., D. Pfaffenbach, and M. D. Davis. 1967. Cell turnover of capillaries. *Lab. Invest.* 17:738–743.

86. Spact, T. H., and I. Lejnieks. 1967. Mitotic activity of rabbit blood vessels. *Proc. Soc. Exp. Biol. Med.* 125:1197–1201.

87. Ausprunk, D. H., and J. Folkman. 1977. Migration and proliferation of endothelial cells in preformed and newly formed blood vessels during tumor angiogenesis. *Microvasc. Res.* 14:53–65.

88. McAllister, K. A., K. M. Grogg, D. W. Johnson, C. J. Gallione, M. A. Baldwin, C. E. Jackson, E. A. Helmbold, D. S. Markel, W. C. McKinnon, J. Murrell, et al. 1994. Endoglin, a TGF-β binding protein of endothelial cells, is the gene for hereditary haemorrhagic telangiectasia type 1. *Nature Genetics.* 8:345–351.